Received: 11 August 2025 | Revised: 15 October 2025 | Accepted: 27 November 2025 | Published online: 12 December 2025

RESEARCH ARTICLE

Archives of Advanced Engineering Science
2026, Vol. 4(2) 148–159
DOI: 10.47852/bonviewAAES52027159

BON VIEW PUBLISHING

Performance Optimization of Multiband Microstrip Antennas Using Support Vector Regression for Wireless Communications

Nejat Abdulwahid Hassen[1], Adomeas Asfaw Tafere[2,*], Murad Ridwan Hassen[1], Tsega Asresa Mengistu[3], Mekete Asmare Huluka[2] and Amsalu Tessema Adgeh[4]

[1]*School of Electrical and Computer Engineering, Addis Ababa University, Ethiopia*

[2]*Department of Electrical and Computer Engineering, Injibara University, Ethiopia*

[3]*Department of Computer Science, Injibara University, Ethiopia*

[4]*Department of Software Engineering, Injibara University, Ethiopia*

Abstract: The increasing demand for compact, high-performance antennas capable of supporting multiple wireless communication standards has driven the development of multiband microstrip antennas. This research presents the design, simulation, and optimization of a multiband microstrip patch antenna operating at 2.4 GHz, 3.5 GHz, and 5.3 GHz, targeting applications in Wi-Fi and WLAN systems. The antenna structure is designed and analyzed using CST Microwave Studio, leveraging its full-wave 3D electromagnetic solver to evaluate key performance metrics including reflection coefficient (S_{11}), gain, bandwidth, and radiation characteristics. To enhance the antenna's performance and reduce the design iteration cycle, support vector regression (SVR), a supervised machine learning technique, is employed. SVR models the nonlinear relationship between the antenna's geometric parameters and its performance outcomes, enabling efficient prediction and optimization. A dataset of 1844 samples is generated through parametric simulations in CST, and the SVR model—using a radial basis function kernel with $C = 300$, $\varepsilon = 0.00000000025$, and $\gamma = 0.5$—is trained to predict return loss and gain across the three target frequencies. The optimized antenna design achieves improved impedance matching, gain enhancement, and bandwidth control at all three frequency bands. Power transfer efficiency exceeds 96% in each band. The results demonstrate that the integration of SVR into the antenna design workflow provides a robust, data-driven approach to achieving multiband performance with high efficiency, making it suitable for next-generation wireless communication systems.

Keywords: multi-band microstrip antenna, support vector regression (SVR), RBF kernel, antenna optimization, machine learning in electromagnetics, CST microwave studio, RF design automation

1. Introduction

In recent years, the explosive expansion of wireless communication technologies has fueled the need for efficient and versatile antenna systems. To ensure smooth connectivity and excellent performance in contemporary communication devices, these systems must support a wide range of standards and operate across several frequency bands [1]. Since multiband antennas enable a single antenna to support multiple communication protocols, such as Wi-Fi, Bluetooth, LTE, WiMAX, and 5G, their development has become a crucial area of research. Microstrip patch antennas have gained significant popularity due to their low profile, ease of integration, and suitability for mass production. Despite their extensive use, particularly for wireless systems that require operation across a wide frequency range, conventional microstrip patch antennas suffer from drawbacks such as narrow bandwidth, low gain, and inadequate multiband performance [2].

Researchers have investigated many design strategies to overcome these obstacles, including the use of slot-loading, fractal geometries, and defective ground structures, all of which aim to increase bandwidth, reduce antenna size, and achieve multiband behavior [3]. Trial-and-error techniques are a major part of the conventional design process for microstrip antennas, often resulting in suboptimal performance and longer design times. Given the complexity of modern wireless systems, it is critical to maintain high-performance standards while streamlining the design process. Optimization methods such as genetic algorithms, particle swarm optimization, and differential evolution provide useful solutions; however, they often require significant computational resources and numerous iterations, which lengthen design cycles.

Recently, machine learning (ML) techniques, particularly support vector regression (SVR), have been applied to antenna design to forecast performance and more efficiently optimize design parameters [3]. SVR is well-suited for solving nonlinear and complex

***Corresponding author:** Adomeas Asfaw Tafere, Department of Electrical and Computer Engineering, Injibara University, Ethiopia. Email: adomeas.asfaw@inu.edu.et

connections between design parameters and antenna performance indicators. By utilizing large datasets generated from electromagnetic simulations, SVR models can accurately predict performance metrics, including return loss, bandwidth, and gain, for various design configurations. This data-driven method speeds up the optimization process and reduces the need for lengthy simulations.

The goal of this research is to maximize the performance of multiband microstrip antennas by combining the strengths of conventional design methods with the power of ML. By using SVR, this study aims to improve the return loss, bandwidth, and gain of the antenna across the specific frequencies of 2.4 GHz, 3.5 GHz, and 5.3 GHz, which are critical for Wi-Fi, WLAN, and ISM band applications. The integration of CST Microwave Studio for electromagnetic simulation and MATLAB for ML-based optimization provides an efficient framework for achieving high-performance antenna designs in less time.

The remainder of this paper is organized as follows:

Section 2 reviews relevant literature and defines key antenna parameters. Section 3 details the proposed antenna geometry and the hybrid methodology combining full-wave simulation and SVR-based optimization, including complete SVR implementation specifications. Section 4 presents and analyzes the simulation results before and after optimization. Section 5 discusses the implications, limitations, assumptions, and potential extensions of this work. Finally, Section 6 concludes the study.

2. Literature Review

Numerous studies have been conducted regarding the design and optimization of multiband microstrip antennas. Below is a selection of notable works.

According to Dai et al. [1], soft computing techniques, specifically SVR, were implemented to expedite the design process of a triple-band microstrip patch antenna, achieving desired performance characteristics. They introduced a novel triple-band antenna structure designed using SVR for the first time, showcasing improved gain values and overall performance compared to existing literature. The effectiveness of the SVR model in significantly reducing design time and providing accurate predictions for resonance frequencies and gain values was demonstrated. The methodology employed wavelet kernel functions, specifically the Mexican-hat wavelet kernel, in the SVR approach for antenna design. Antenna patch dimensions, substrate properties, and parametric analysis data were used to compute feed locations, slot positions, and antenna characteristics. The SVR model parameters, including the kernel function and related hyperparameters, were selected and implemented in MATLAB for training and testing the model.

Traditional trial-and-error methodologies in antenna design have long been criticized for their inefficiency and lack of precision. Early experimental approaches, characterized by iterative physical prototyping and manual adjustments, often resulted in suboptimal designs and prolonged development cycles [4]. This inefficiency has driven researchers to seek more systematic and computational methods to overcome the inherent limitations of conventional practices [5].

The need for antennas that can function across several frequency bands has grown dramatically as a result of the quick development of wireless communication technology. The many performance needs of modern applications like GSM, Wi-Fi, and WLAN cannot be satisfied by traditional single-band antennas. Extensive study on multiband designs that can sustain several resonant modes in a single compact structure at the same time has been prompted by this expanding requirement [6].

To address the challenges associated with multiband operation, researchers have increasingly turned to simulation-based methodologies. Advanced electromagnetic simulation tools like CST Microwave Studio offer high-fidelity, three-dimensional modeling capabilities, allowing designers to assess antenna performance under various conditions [7]. These platforms provide rapid feedback on design modifications, significantly reducing the need for physical prototypes.

An effective method for forecasting electromagnetic behavior in recent years has been the incorporation of ML techniques into antenna design. In particular, SVR has been effectively used to describe the nonlinear correlations between the performance metrics and the physical characteristics of an antenna. Researchers can reduce the computational cost of full-wave simulations by using SVR to forecast important performance metrics, including resonance frequencies, return loss, and gain, with remarkable accuracy.

Material selection and substrate properties play a critical role in determining an antenna's performance. The use of FR-4, for example, has been extensively documented for its moderate dielectric constant, cost-effectiveness, and ease of availability, making it a popular choice for low-frequency applications [8]. The substrate not only influences resonant frequencies but also affects bandwidth and radiation efficiency, emphasizing the need for careful material consideration during design.

Slotting techniques have garnered considerable attention as a means to introduce additional resonant modes into microstrip antennas [9]. By incorporating slots, whether symmetrical, asymmetrical, or randomly distributed, researchers have demonstrated the creation of multiple current paths on the radiating patch, enabling multiband operation [10]. This approach has proven particularly effective in compact designs where space constraints demand innovative methods to achieve desired frequency responses.

Comparative studies on slot geometries reveal that rectangular slots often provide significant advantages over alternative shapes such as circular or U-shaped slots. The simplicity of rectangular slots facilitates easier integration into standard PCB manufacturing processes, while their predictable impact on current distribution makes them highly effective for performance enhancement [11]. The consensus in the literature indicates that rectangular slotting strikes a favorable balance between design complexity and electromagnetic performance.

Advanced electromagnetic simulation tools are indispensable in modern antenna design, enabling precise validation of theoretical models and iterative refinement of design parameters. Platforms like CST Microwave Studio have revolutionized the design process by allowing detailed three-dimensional analysis that closely mirrors real-world conditions [12]. This high level of simulation accuracy has substantially reduced reliance on physical prototyping, saving both time and resources.

An important paradigm shift in antenna design is represented by the combination of evolutionary optimization and ML [13]. Designers can quickly settle on high-performance configurations that satisfy exacting design requirements by fusing the predictive strength of SVR with the reliable search capabilities of optimization algorithms [14]. This hybrid technique improves the final antenna configuration's durability while speeding up the design period.

Recent studies have demonstrated the effectiveness of hybrid methodologies that merge classical electromagnetic theory with modern computational techniques [15]. These interdisciplinary approaches have allowed researchers to tackle complex design problems by leveraging both theoretical insights and advanced data-driven methods. The synergy between traditional and contemporary

techniques has opened new avenues for innovation in multiband antenna design, enabling the creation of structures that are both high-performing and manufacturable [16].

2.1. Antenna parameters and SVR algorithm

To evaluate the performance of an antenna, it is important to outline several key parameters. Many of these parameters are connected to one another, and providing all of them is not always required for a full characterization of the antenna's behavior. This section will present the definitions of these parameters [17].

2.1.1. Radiation pattern

An antenna radiation pattern, also known as an antenna pattern, describes how an antenna radiates energy in space and can be expressed either through mathematical equations or graphical illustrations based on spatial coordinates [17]. Typically, this pattern is analyzed in the far-field zone and shown as a function of directional angles. The radiation characteristics include parameters such as power flux density, radiation intensity, field strength, directivity, phase, and polarization [17]. Among these, the main focus is usually on how the radiated energy is distributed in space in two or three dimensions, depending on the observer's position at a fixed distance from the antenna. Figure 1 [17] displays a common choice of coordinate system for this purpose. When plotting the variation of the received electric (or magnetic) field at a constant distance, it is referred to as the amplitude field pattern. Conversely, when showing how the power density changes spatially at a fixed radius, the result is known as the amplitude power pattern [18]. The field and power patterns are often expressed in a normalized form by scaling them with respect to their maximum value. Additionally, the power pattern is generally displayed using a logarithmic scale, most commonly in decibels (dB). This approach is beneficial because it provides a clearer view of portions of the pattern with very small values, which will be identified later as minor lobes [17]. In the case of an antenna:

- A field pattern (on a linear scale) illustrates how the magnitude of the electric or magnetic field varies with angle in space.

Figure 1
Antenna analysis coordinate system

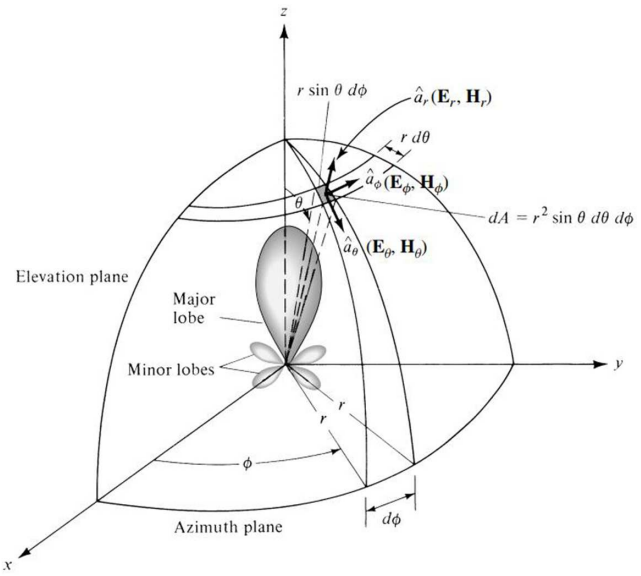

- A power pattern (on a linear scale) shows how the square of the electric or magnetic field's magnitude changes with angular position.
- A power pattern (in dB) presents the electric or magnetic field's magnitude in decibel units as it depends on the angular position.

2.1.2. Return loss

It is a parameter used to measure the power reflected by the antenna due to an improper matching between the transmission line and antenna [17]. Return loss, like voltage standing wave ratio (VSWR), indicates how well the matching between the transmitter and receiver has been achieved. It describes the ratio of the power in the reflected wave to the power in the incident wave, expressed in dB [17]. The return loss is given by:

$$Return\ Loss = 20 \log |\gamma| \ (dB) \tag{1}$$

where $|\gamma|$ represents the magnitude of the reflection coefficient, and this value is always less than or equal to 1. For ideal matching between the transmitter and the receiver, $|\gamma| = 0$, and $RL = \infty$, which implies that no power is reflected back. Conversely, when $|\gamma| = 1$, $RL = 0$ dB, indicating that the antenna radiates no power because all the power supplied to the antenna is completely reflected.

2.1.3. S-parameters

The *S*-parameters are very important in microwave design for describing the behavior of electrical devices. Most electrical properties such as VSWR, return loss, and gain are related to the *S*-parameters. *S*-parameters characterize the input and output relationships between ports in an electrical system. Specifically, S_{11} and S_{22} represent the input and output reflection coefficients, while S_{21} is the forward transmission coefficient (gain), and S_{12} is the reverse transmission coefficient (isolation), which measures the power transferred from port 1 to port 2 [19]. S_{11} (sometimes referred to as return loss) represents how much power is reflected from the antenna and is therefore known as the reflection coefficient. If $S_{11} = 0$ dB, all the power is reflected from the antenna, and nothing is radiated.

2.1.4. Directivity

The directivity of an antenna is one of the most important parameters in this work because antennas will be compared using this figure of merit. According to the definition provided by Saeed [20], directivity is the ratio between the radiation intensity in a specific direction from the antenna and the average radiation intensity over all directions. The average radiation intensity, denoted as U_0, is calculated by dividing the total power radiated by the antenna by 4π, which corresponds to the radiation intensity of an ideal isotropic radiator. This relationship can be mathematically expressed as:

$$D(\theta, \phi) = 4\pi \frac{U(\theta, \phi)}{U0} \tag{2}$$

In this context, D denotes the directivity of the antenna, U is the antenna's radiation intensity, U_0 represents the radiation intensity of an ideal isotropic radiator, and Prad is the total power emitted by the antenna. Since directivity is defined as the ratio between two radiation intensities, it is a dimensionless measure. For convenience, it is often expressed in dB. The directivity provides insight into how the antenna's radiated power is distributed in space, highlighting directions where the radiation is stronger or weaker relative to an isotropic source. Antennas with a narrower primary lobe exhibit higher directivity compared to those with broader lobes, making them more focused in their radiation pattern.

2.1.5. Gain

The gain is defined as the ratio of the radiation intensity, in a given direction, to the radiation intensity that would be obtained if the power accepted by the antenna were transmitted isotropically. It is noted that this definition is closely related to directivity, with the key difference being that gain considers the conduction and dielectric efficiencies.

2.1.6. Antenna efficiency

During the design and measurement phases, antenna characteristics are crucial for defining antenna performance. This section provides a thorough review of antenna behavior by explaining several important parameters. Directivity, bandwidth, radiation pattern, gain, efficiency, input impedance, return loss, and *S*-parameters are among the key factors considered. Each of these variables plays a vital role in understanding and improving antenna performance across various communication applications. The following explanations explore the nuances of these properties, providing insight into their functions and implications within the field of antenna engineering. Next, the total efficiency of an antenna is defined as follows [17]:

$$e_o = e_r e_c e_d \tag{3}$$

where

- e_0 = total efficiency
- e_r = reflection (mismatch)efficiency
- e_c = conduction efficiency
- e_d = dielectric efficiency

The antenna's radiation efficiency is the product of conduction efficiency and dielectric efficiency. The losses, known as I^2R losses, are due to conduction and dielectric effects.

2.1.7. Bandwidth

Antenna bandwidth refers to the frequency range over which the antenna meets certain specified performance criteria related to characteristics such as input impedance, radiation pattern, or gain. Typically, this range is centered on a particular frequency, like the resonant frequency for dipole antennas. For broadband antennas, bandwidth is often represented by the ratio of the highest to the lowest usable frequencies. In contrast, for narrowband antennas, it is commonly given as a percentage, calculated by dividing the frequency difference between the upper and lower limits by the center frequency, as shown in (4) [17].

$$BW = 100\ \frac{FH - FL}{FC} \tag{4}$$

where

- *FH* is the highest frequency,
- *FL* is the lowest frequency
- *FC* is the center frequency in the band

2.1.8. Designing of conventional microstrip patch antenna

Designing a patch antenna involves determining the physical dimensions and material properties needed to achieve the desired resonant frequency and radiation performance. The process begins by selecting a suitable dielectric substrate with a known relative permittivity and thickness, as these factors influence the antenna's bandwidth and efficiency. Using design equations, the width and length of the patch are calculated based on the target operating frequency, typically in the microwave range. These calculations account for the effects of the substrate and fringing fields. Additional considerations include the feeding method (such as microstrip line, coaxial probe, or inset feed) to ensure proper impedance matching, typically to 50 ohms. The geometry of the triband microstrip antenna is shown in Figure 2.

Figure 2
Triband microstrip antenna design

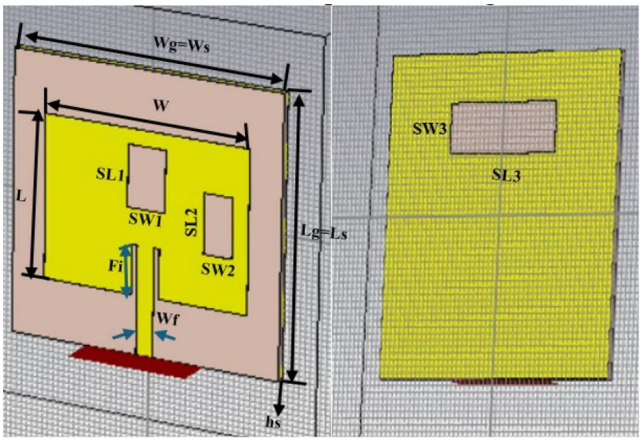

1) Top View (Radiating Patch)

The left image shows the main patch structure printed on a dielectric substrate. The key geometrical parameters are labeled as follows:

- *L* and *W*: Represent the length and width of the main patch, respectively. These determine the fundamental resonant frequency of the antenna.
- $W_g = W_s$ and $L_g = L_s$: Denote the substrate or ground dimensions, chosen to ensure proper field confinement and minimize edge effects.
- h_s: Indicates the substrate height, which affects impedance matching and bandwidth.

The patch incorporates two rectangular slots (*SL1* and *SL2*) with widths *SW1* and *SW2*, respectively. These slots are strategically cut into the main patch to introduce additional current paths. By doing so, they modify the effective electrical length of the antenna, enabling it to resonate at multiple frequencies.

- *SL1* primarily influences the lower resonant frequency around 2.4 GHz.
- *SL2* adjusts the second resonant mode, typically contributing to the mid-band resonance at 3.5 GHz.

2) Bottom View (Ground Plane)

The right image displays the ground plane configuration. The ground plane includes a rectangular slot (*SL3*) of width *SW3*, which is cut into it. This slot interacts electromagnetically with the patch and feed line, further tuning the antenna's impedance and resonance characteristics.

- *SL3* helps excite an additional resonance, usually contributing to the third frequency band 5.3 GHz.
- The placement and size of *SL3* alter the current distribution on the ground plane, improving impedance bandwidth and inter-band isolation.

3) Multiband Operation

The combination of the three slots (*SL1*, *SL2*, and *SL3*) allows the antenna to operate in triband mode.

- Each slot perturbs the surface current path differently, effectively increasing the number of resonant modes supported by the patch.
- The interaction between these slots enables fine-tuning of resonant frequencies and impedance matching at 2.4 GHz, 3.5 GHz, and 5.3 GHz, commonly used for Wi-Fi, WiMAX, and WLAN applications.

The feed line coupling, slot dimensions, and slot placement are optimized to achieve good return loss, gain, and radiation efficiency at all three bands.

2.1.9. Support vector regression model (SVR)

SVR is a powerful regression technique derived from support vector machine theory, designed to predict continuous output values by identifying an optimal hyperplane in a high-dimensional feature space that best fits the training data within a specified tolerance margin [21]. Unlike conventional regression models that minimize squared errors, SVR employs an ε-insensitive loss function that ignores errors smaller than ε, promoting robustness against noise and overfitting. The SVR model used in this study employs a radial basis function (RBF) kernel, defined as:

$$K\left(x_i, x_j\right) = e^{(-\gamma \left\|x_i - x_j\right\|^2)} \tag{5}$$

where $\gamma = 0.5$ controls the influence of individual training samples. The regularization parameter $C = 300$ balances model complexity and training error tolerance, while the tube width $\varepsilon = 0.00000000025$ defines the margin of acceptable prediction deviation. The input feature vector x consists of eight geometric parameters:

$$x = [SL1,\ SL2,\ SL3,\ SW1,\ SW2,\ SW3,\ h_s,\ F_i] \tag{6}$$

where SL and SW denote the slot lengths and widths, h_s is the substrate height, and F_i is the inset feed depth. The output targets y include six performance metrics:

$$\begin{aligned} y = [&S_{11}@2.4GHz,\ S_{11}@3.5GHz,\ S_{11}@5.3GHz,\\ &Gain\ @2.4\ GHz,\ Gain@3.5GHz,\ Gain@5.3GHz] \end{aligned} \tag{7}$$

A dataset of 1844 samples was generated via parametric sweeps in CST Microwave Studio, varying the input parameters within physically realizable bounds. The dataset was randomly split into 80% training (1475 samples) and 20% testing (369 samples), with 5-fold cross-validation applied during hyperparameter tuning to ensure generalization.

Model performance was evaluated using the coefficient of determination ($R^2 > 0.94$ for all outputs) and root mean squared error ($RMSE < 0.8$ dB for S_{11} predictions). The trained SVR model serves as a fast surrogate, replacing computationally expensive full-wave simulations during optimization.

3. Proposed Design and Optimization Framework

3.1. Research design

The design process of a multiband microstrip patch antenna involves an organized and incremental process combining electromagnetic simulation and ML techniques. The process begins with defining the design parameters. To be specific, the desired frequency bands for multiband operation are identified—starting with 2.4 GHz as an initial guess. With these target frequencies and antenna size constraints, an appropriate substrate material and its dimensions are selected to screen physical realizability and electromagnetic compatibility.

An initial antenna design is simulated with CST Microwave Studio. This initial design focuses on achieving minimum functionality and is simulated to identify key performance parameters such as return loss, gain, and resonant frequency. For multiband operation, slots are added in the patch antenna. Slotting enhances the performance by supporting multiple resonant modes and impedance matching. In this configuration, three slots are added—two on the patch and one on the ground plane. Such a planned allocation offers huge advantages over all the slots being added to the patch. A ground plane slot, for example, can introduce new modes of resonance with reduced interference to patch currents, thereby enabling wider bandwidth and better impedance tuning. It also enhances radiation pattern control and reduces current disturbances and ultimately leads to greater gain and efficiency.

One important step subsequent to the initial design is data capture for training an SVR model. A number of simulations are run in CST as the different parameters, such as slot dimensions, substrate thickness, and feed positions, are varied. The resulting simulations yield datasets that contain a relationship between design parameters and performance outcomes, namely, *S*-parameters (for return loss) and realized gain at particular frequencies. The datasets obtained are exported for analysis and modeling in MATLAB.

In MATLAB, the SVR model is trained to predict antenna performance from data collected with CST simulations. Definition of design variables, for example, slot width and length, and the performance parameters like resonant frequency, return loss (S_{11}), and gain are initialized in the first place and then activated in the optimization process. The SVR model is employed as a surrogate predictor enabling fast computation of new designs without the need to conduct computationally heavy full-wave simulations. A cost function is created from these SVR predictions to balance many opposing objectives, for example, minimizing return loss and maximizing gain. Optimization solvers like fmincon are used to find the optimum set of design parameters to meet these needs. The cost function typically takes the form of a weighted sum so that particular performance requirements can be preferred, for example, S_{11} being below –10 dB and a large gain in the target frequency bands.

When optimal parameters are determined, they are re-imported into CST to redesign the antenna. The procedure is then iteratively repeated with one more simulation to verify the accuracy of the model and to determine whether the predicted gain improvements, return loss, and frequency alignment have been made. When observed inaccuracies are present, the loop is repeated—new simulation data are added to the training set, the SVR model is retrained, and the optimization is repeated. This repeated optimization ensures that the final antenna design is not only theoretically optimal but also a validated design from high-fidelity electromagnetic simulations.

The flow chart in Figure 3 illustrates the systematic process of designing and optimizing a microstrip antenna for triband operation. The process begins with selecting the desired operating frequency, followed by choosing a suitable substrate material based on its dielectric constant and height. Next, the key antenna parameters are determined, and an initial design with a 50-ohm feed line is created using CST software. The antenna is then simulated to achieve performance near the target frequency of 2.4 GHz. To enable triband operation, slots are introduced into the antenna structure, and further simulations and parametric analyses are conducted to achieve resonant frequencies at 2.4 GHz, 3.5 GHz, and

Figure 3
System modeling flow chart

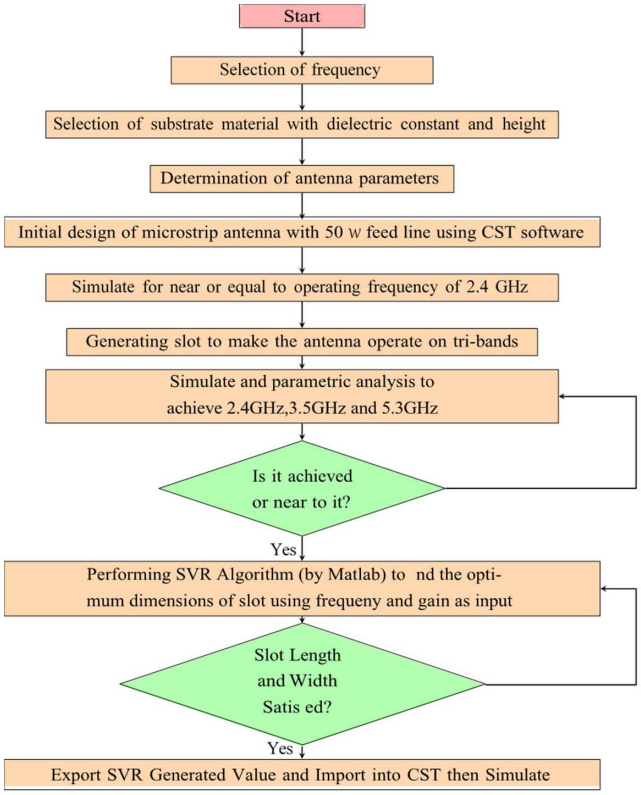

Figure 4
SVR flow chart

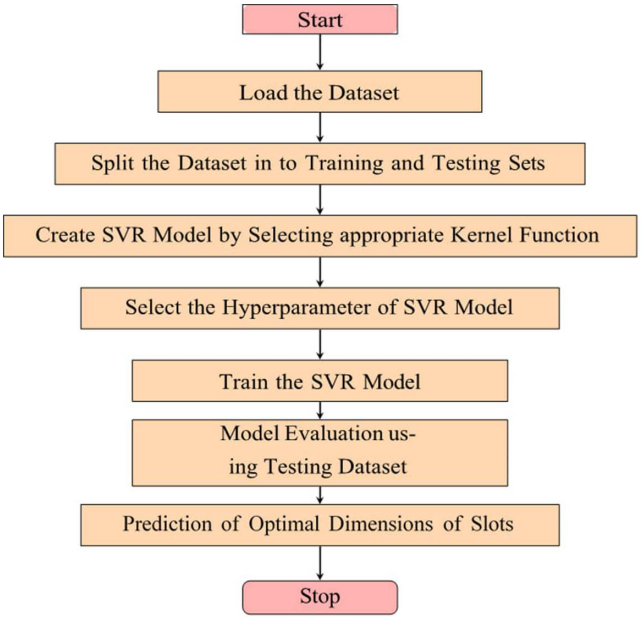

5.3 GHz. If the desired frequency responses are not obtained, the design parameters are adjusted iteratively. Once the target frequencies are achieved or closely matched, an SVR algorithm in MATLAB is employed to optimize the slot dimensions using frequency and gain as input parameters. The optimized slot length and width are then evaluated for satisfaction. If the results are satisfactory, the SVR-generated values are exported and imported back into CST software for final simulation and validation, completing the antenna design and optimization process.

The flow chart in Figure 4 depicts a systematic ML workflow designed to predict optimal slot dimensions using SVR. The process begins by loading a dataset containing relevant input features and target values, which is then split into training and testing subsets to facilitate model development and unbiased evaluation. An SVR model is created by selecting the RBF kernel function. Following this, key hyperparameters (C = 300, ε = 0.00000000025, γ = 0.5) are carefully tuned via grid search. The model is then trained on the training data to learn the underlying relationship between inputs and slot dimensions. After training, the model's predictive accuracy and generalization capability are assessed using the held-out testing dataset, typically through metrics like RMSE, mean absolute error (MAE), or R^2. Once validated, the model is used to predict the optimal dimensions of slots for new input conditions, providing actionable insights for engineering or manufacturing applications. The workflow concludes after successful prediction, representing a complete end-to-end pipeline from data ingestion to practical output.

4. Simulation Results

CST Microwave Studio, a 3D electromagnetic simulation tool, is used to model and simulate the performance of the designed microstrip patch antenna. The key design parameters are listed in Table 1.

Table 1
Key design parameters for microstrip patch antenna

Parameter	Value
W	38
L	29
W_g	50
L_g	50
H_g	0.035
W_f	3.137
F_i	8.85
ϵ_r	4.4
H_s	1.6

*Note: All dimensional parameters are in millimeters (mm); ϵ_r is dimensionless.

Where:

- W and L are the patch width and length.
- W_g and L_g are the ground width and length.
- H_g is the thickness of metallic material.
- ϵ_r is the dielectric constant.
- W_f is the width of the microstrip feed.
- F_i is the depth of inset.
- H_s is the height of substrate.

4.1. Return loss results

As a result of the simulation, the S-parameter analysis of the optimized multiband microstrip patch antenna, represented by Figure 5, demonstrates a significant return loss performance improvement after optimization. Prior to optimization, measured

Figure 5
Return loss results before and after optimization

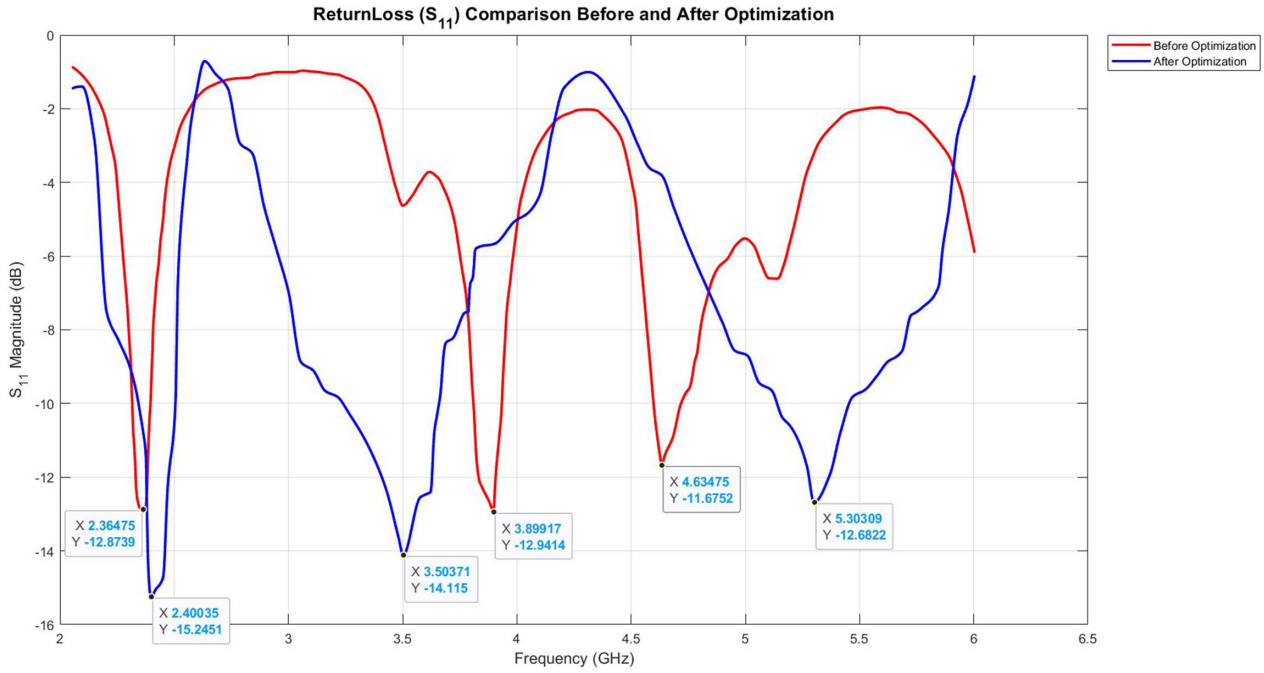

return loss was recorded for three resonating frequencies of 2.36475 GHz, 3.8991 GHz, and 4.6347 GHz with respective return loss values of –12.8739 dB, –12.9414 dB, and –11.6752 dB. After the optimization process—guided by the (SVR model—the antenna achieved improved return loss readings of –15.2451 dB at 2.4 GHz, –14.115 dB at 3.5 GHz, and –12.682 dB at 5.3 GHz. These results validate that optimization enhanced the antenna's performance by aligning the resonant frequencies precisely with the target bands and reducing return loss across all three frequency points. The power transfer efficiency (η), calculated as $\eta = 1 - |S_{11}|^2$, exceeds 96% at each band, confirming excellent impedance matching.

4.2. Gain results

4.2.1. Frequency of 2.4 GHz

Figures 6 and 7 present polar plots of the far-field directivity patterns of the antenna before and after optimization. The plots indicate radiation characteristics as a function of polar angle θ ($0° \leq \theta \leq 180°$) in the azimuth plane, with the elevation angle set equal to $\phi = 90°$. Both plots are an operating frequency of 2.4 GHz and are designed to graphically illustrate the direction performance of the antenna. The polar angle θ in degrees is on the x-axis, and the magnitude of radiation in dB relative to an isotropic radiator (dBi) is on the y-axis. Comparative study of the two figures reveals differences in gain pattern and directivity of the antenna before and after optimization. Generally, as shown in Figures 6 and 7, post-optimization gain improved from 5.75 to 5.81 dBi.

4.2.2. Frequency of 3.5 GHz

Figures 8 and 9 (before and after optimization) are polar plots of the far-field directivity patterns of an antenna at a constant frequency of 3.5 GHz with a constant elevation angle of $\phi = 90°$. In the first graph (before optimization), the main lobe peak occurs at $\theta = 149°$ with a magnitude of 6.24 dBi, and secondary lobes are visible, particularly around $\theta = 180°$, where the radiation level drops significantly before rising again. The peak of the main lobe moved slightly to $\theta = 147°$ with a value of 6.33 dBi, and the same pattern of principal declines and increases can be observed around $\theta = 180°$ in the second plot.

Overall, after optimization, the main lobe gain increases marginally from 6.24 to 6.33 dBi, a marginal increase in efficiency or directivity, and the main lobe direction shifts by 2°, which may be significant depending on the application. The beam width increases marginally from 59.5° to 60.1°, which means a broader main lobe and a potential trade-off between side lobe suppression and directivity. Most noticeable is the enhancement of side lobe levels from –1.2 dB to –3.5 dB, illustrating better suppression of unwanted directions of radiation, which works to reduce interference and enhance overall antenna performance. Generally, as shown in Figures 8 and 9, the main lobe gain increased from 6.24 to 6.33 dBi, with improved side lobe suppression (from –1.2 to –3.5 dB).

4.2.3. Frequency of 5.325 GHz

Figures 10 and 11 present polar plots of the far-field directivity patterns of the antenna at 5.325 GHz for an elevation angle of $\phi = 90°$, pre-optimization, and post-optimization. Without any optimization, the maximum value of the main lobe takes place at $\theta = 23°$ with a gain of 2.58 dBi and possesses secondary lobes at $\theta = 180°$. On optimization, the center lobe shifts to $\theta = 13°$ with a gain of 4.4 dBi, while the secondary lobes are at nearly the same positions. Beam width reduces significantly from 231.0° to 63.7°, indicating improved directivity, but side lobe level remains unchanged at –1.1 dB. Generally, as shown in Figures 10 and 11, the gain improved dramatically from 2.58 to 4.4 dBi, and the beam width narrowed from 231.0° to 63.7°, indicating significantly enhanced directivity.

Figure 6
Polar plot of far-field directivity at 2.4 GHz before optimization

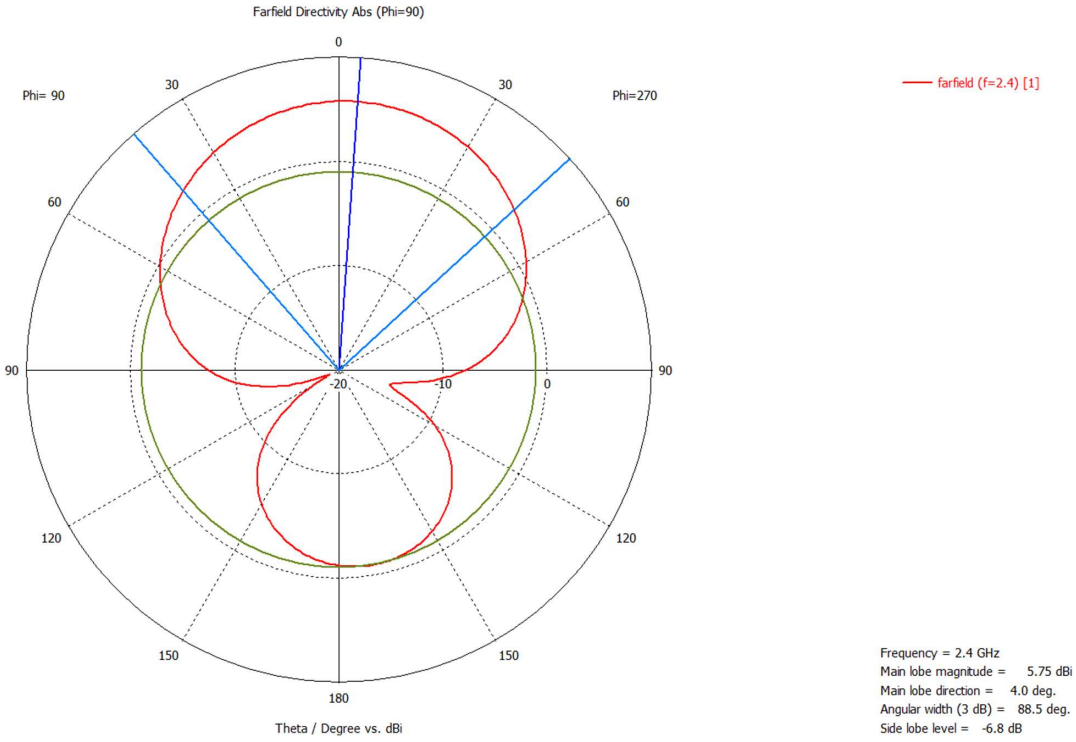

Figure 7
Polar plot of far-field directivity at 2.4 GHz after optimization

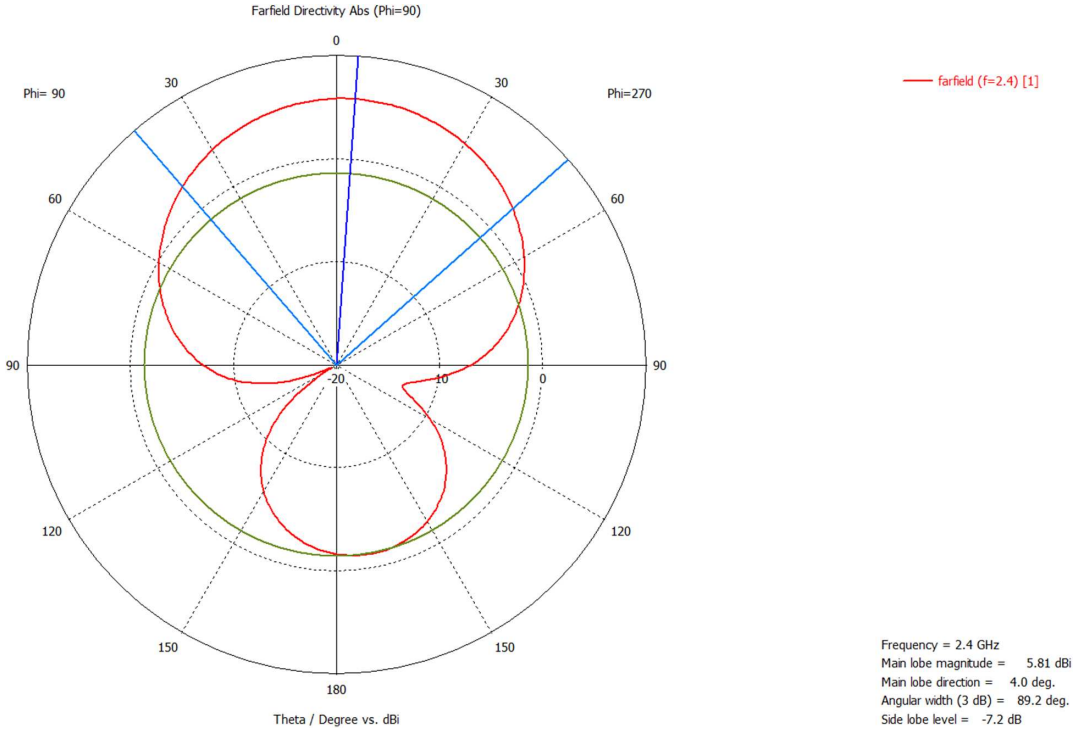

Figure 8
Polar plot of far-field directivity at 3.5 GHz before optimization

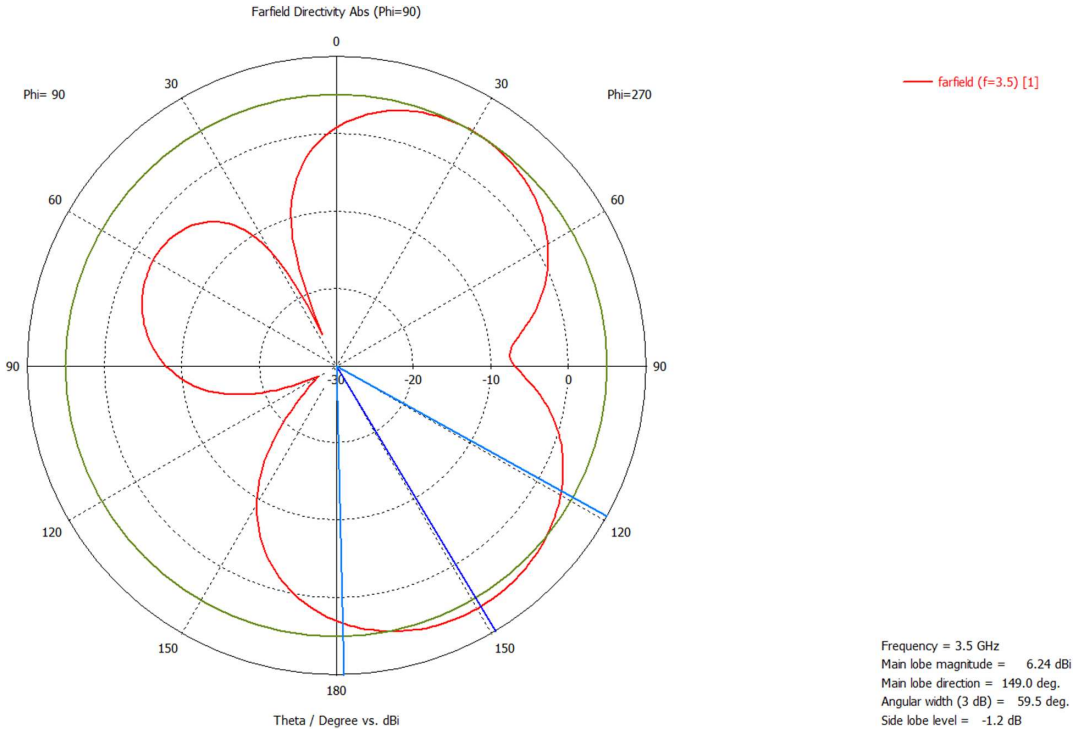

Figure 9
Polar plot of far-field directivity at 3.5 GHz after optimization

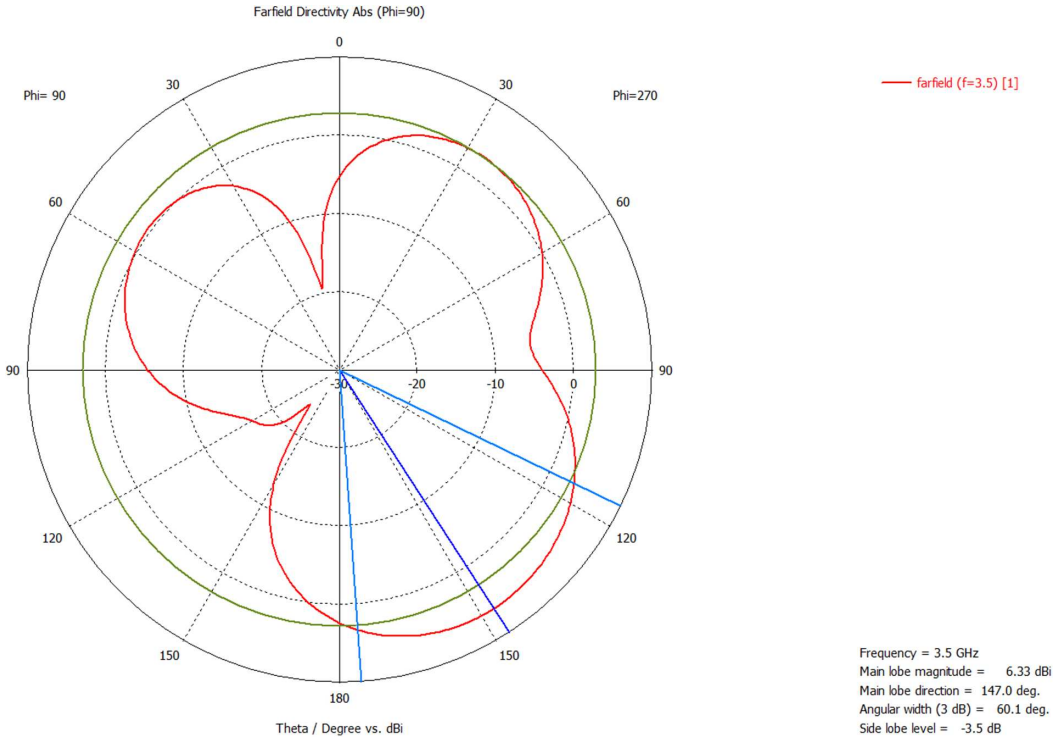

Figure 10
Polar plot of far-field directivity at 5.325 GHz before optimization

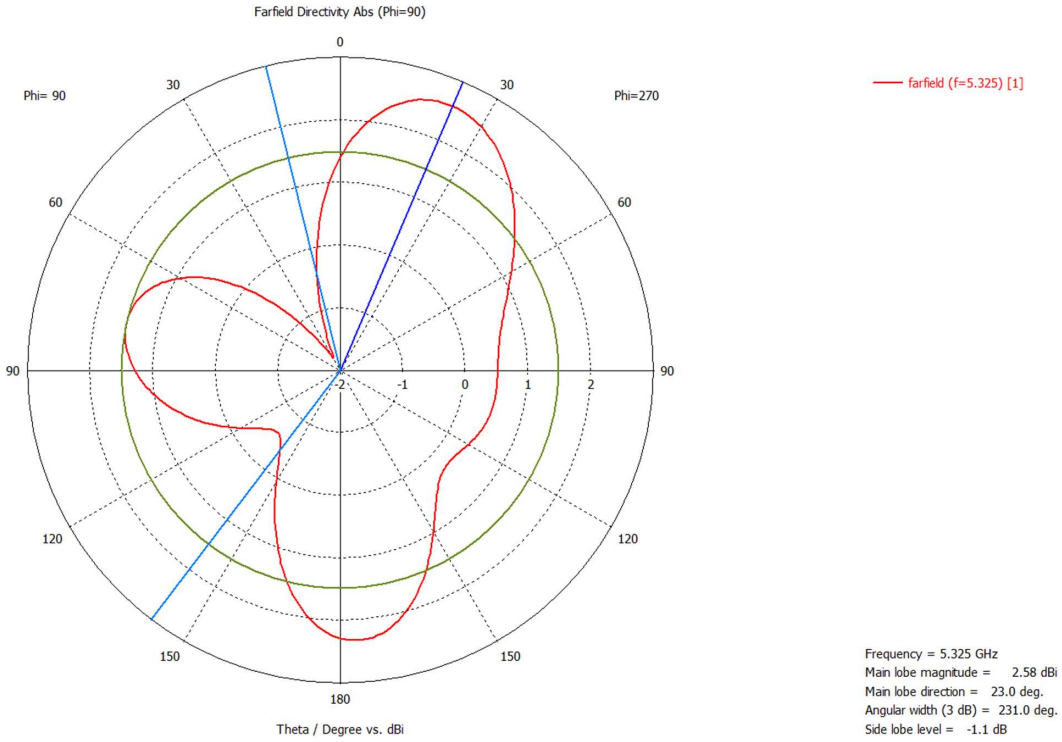

Figure 11
Polar plot of far-field directivity at 5.325 GHz after optimization

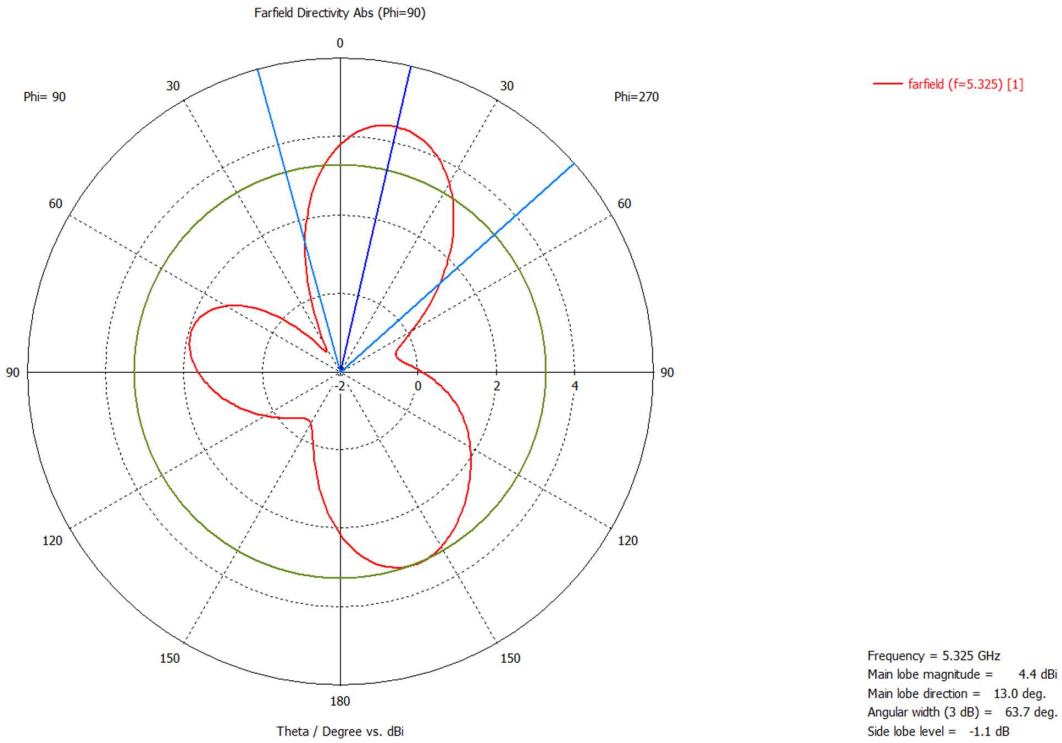

5. Discussion

The SVR-optimized multiband microstrip patch antenna demonstrates considerable improvement in the key performance metrics. The return loss at required frequencies was improved from –12.87, –12.94, and –11.67 dB (2.36, 3.89, and 4.63 GHz) to –15, –14, and –12.6 dB (2.4, 3.5, and 5.3 GHz), all below the –10 dB level, indicating good impedance matching. Respective bandwidths increased from 50.5, 70.2, and 80.1 MHz to 65.5, 90.3, and 101.4 MHz, meeting the requirements of Wi-Fi, WiMAX/5G, and ISM applications, respectively. Antenna gain was moderately increased at 2.4 GHz (5.75 → 5.81 dBi) and 3.5 GHz (6.24 → 6.33 dBi) and highly at 5.325 GHz (2.58 → 4.4 dBi).

5.1. Limitations

This study is based entirely on electromagnetic simulations and does not include physical prototyping or real-world testing. The design assumes an ideal FR-4 substrate with uniform permittivity and neglects manufacturing tolerances, thermal effects, and mutual coupling in array configurations. Additionally, the SVR model is trained solely on simulated data; real-world variations (e.g., soldering imperfections, material inhomogeneity) may affect performance.

6. Conclusion

In this research, a multiband microstrip antenna was designed, analyzed, and optimized to satisfy the rising needs of today's wireless communication networks. The antenna demonstrated effective operation across key frequency bands, including 2.4 GHz, 3.5 GHz, and 5.3 GHz, making it suitable for applications such as Wi-Fi and WLAN communication. To address the inherent limitations of conventional design approaches, SVR was employed as a predictive and optimization tool. By training the SVR model on a dataset generated through parametric electromagnetic simulations, we were able to accurately predict key performance metrics such as return loss, bandwidth, and gain. The SVR-guided optimization led to substantial improvements, including enhanced return loss, increased bandwidth, and more uniform gain across the targeted bands. The integration of SVR into the antenna design process proved to be both efficient and effective, reducing the need for time-consuming simulation iterations and enabling faster convergence to optimal design solutions. This approach highlights the potential of ML in radio frequency (RF) and antenna engineering, particularly for complex, multi-objective design problems.

Recommendations

Further investigations should focus on conducting detailed sensitivity analyses to quantify the impact of variations in slot dimensions, placements, and substrate parameters. This analysis will help in understanding the robustness of the design and establishing acceptable tolerance limits for mass production. Although FR-4 is cost-effective and widely used, exploring alternative substrates with lower loss tangents or higher dielectric stability could potentially enhance antenna performance, especially for high-frequency or high-data-rate applications. Future work may benefit from exploring the integration of additional ML models or metaheuristic strategies. Such methods could further refine the optimization process by improving convergence speed and global optimality, thereby enhancing the overall design quality. To further streamline the design process, integrating the optimization framework with automated design and prototyping tools is advisable. This integration would facilitate real-time performance predictions and enable rapid iteration of design modifications, enhancing both the throughput and quality of antenna designs for commercial applications. Incorporating a comprehensive multi-objective optimization strategy that explicitly considers and balances trade-offs among key design metrics (bandwidth, gain, cost, and manufacturability) would provide designers with a spectrum solution. This approach would enable more informed decisions tailored to specific application requirements. Overall, future works may include:

- Fabrication and over-the-air measurement of the prototype,
- Sensitivity analysis of geometric parameters,
- Comparison with other ML models (e.g., XGBoost, convolutional neural networks (CNNs)),
- Exploration of low-loss substrates (e.g., Rogers RO4003),
- Extension to MIMO or array configurations.

Ethical Statement

This study does not contain any studies with human or animal subjects performed by any of the authors.

Conflicts of Interest

The authors declare that they have no conflicts of interest to this work.

Data Availability Statement

Data are available from the corresponding author upon reasonable request.

Author Contribution Statement

Nejat Abdulwahid Hassen: Conceptualization, Methodology, Software, Validation, Formal analysis, Investigation, Data curation, Writing – original draft, Visualization, Supervision. **Adomeas Asfaw Tafere:** Conceptualization, Methodology, Software, Validation, Resources, Data curation, Writing – review & editing, Visualization, Supervision. **Murad Ridwan Hassen:** Conceptualization, Methodology, Software, Formal analysis, Investigation, Resources, Writing – original draft, Visualization, Supervision, Project administration. **Tsega Asresa Mengistu:** Conceptualization, Software, Validation, Resources, Writing – review & editing, Visualization, Supervision. **Mekete Asmare Huluka:** Conceptualization, Software, Validation, Resources, Writing – review & editing, Visualization, Supervision. **Amsalu Tessema Adgeh:** Conceptualization, Software, Formal analysis, Resources, Writing – review & editing, Visualization.

References

[1] Dai, X. W., Mi, D. L., Wu, H. T., & Zhang, Y. H. (2022). Design of compact patch antenna based on support vector regression. *Radio Engineering*, *31*(3), 339–345. https://doi.org/10.13164/RE.2022.0339

[2] Chen, Y., Elsherbeni, A. Z., & Demir, V. (2022). Machine learning for microstrip patch antenna design: Observations and recommendations. In *Proceedings of the 2022 United States National Committee of URSI National Radio Science Meeting (USNC-URSI NRSM)*, 256–257.

[3] Tafere, A. A., Hailemariam, T. S., & Debella, T. T. (2025). Deep Learning-Powered Equalization with Autoencoders for Improved 5G Communication. In *2025 IEEE International Conference on Interdisciplinary Approaches in Technology and Management for Social Innovation (IATMSI)*, *3*, 1–6. IEEE. https://doi.org/10.1109/IATMSI64286.2025.10984954

[4] Narumi, K., Shi, X., Hodges, S., Kawahara, Y., Shimizu, S., & Asami, T. (2015). Circuit eraser: A tool for iterative design with conductive ink. In *Proceedings of the 18th ACM Conference on Human Factors in Computing Systems*, 2307–2312. https://doi.org/10.1145/2702613.2732876

[5] Kaşas, S., Faraji-Dana, R., Shahabadi, M., & Safavi-Naeini, S. (2020). A fast-computational method for characteristic modes and eigenvalues of array antennas. *IEEE Transactions on Antennas and Propagation*, *68*(12), 7879–7892. https://doi.org/10.1109/TAP.2020.3000566

[6] Rasool, J. M., & Abd, A. K. (2024). A reconfigurable antenna for IoT applications with enhanced performance by adding metamaterial. *Journal of Communications*, *19*(4), 198–203. https://doi.org/10.12720/jcm.19.4.198-203

[7] Du, Y., Zhao, D., Guo, C., He, J., Yao, H., Zou, J., & Z, Wang, B. (2025). Continuous spatio-temporal synthesis of electromagnetic fields by projected space-time Fourier transform. *Communications Engineering*, *16*(1), Article 110. https://doi.org/10.1038/s44172-025-00448-9

[8] Singh, J., & Lal Lohar, F. (2020). Frequency reconfigurable quad band patch antenna for radar and satellite applications using FR-4 material. *Materials Today: Proceedings*, *28*, 2026–2030. https://doi.org/10.1016/j.matpr.2020.05.609

[9] Deshmukh, A., & Ray, K. P. (2015). Analysis of broadband variations of U-slot cut rectangular microstrip antennas. *IEEE Antennas and Propagation Magazine*, *57*(2), 181–193. https://doi.org/10.1109/MAP.2015.2414533

[10] Ossa-Molina, O., & López-Giraldo, F. (2022). A simple model to compute the characteristic parameters of a slotted rectangular microstrip patch antenna. *Electronics*, *11*(1), 129. https://doi.org/10.3390/electronics11010129

[11] Aftanasar, M. S., & Hafiz, M. N. (2016). "Fabricated multilayer SIW system using PCB manufacturing process,". In *Proceedings of IEEE Asia-Pacific Conference on Applied Electromagnetics (APACE)*, 100–104. https://doi.org/10.1109/APACE.2016.7915861

[12] Khabbat Ezzulddin, S., Hasan, S. O., & Ameen, M. M. (2020). Design and simulation of microstrip patch antenna for 5G application using CST Studio. *International Journal of Advanced Science and Technology*, *29*(4), 7193–7205.

[13] Wu, Q., Cao, Y., Wang, H., & Hong, W. (2020). Machine-learning-assisted optimization and its application to antenna designs: Opportunities and challenges. *China Communications*, *17*, 152–164. https://doi.org/ 10.23919/JCC.2020.04.014

[14] Sarker, N., Podder, P., Mondal, M. R. H., Shafin, S. S., & Kamruzzaman, J. (2023). Applications of machine learning and deep learning in antenna design, optimization, and selection: A review. *IEEE Access*, *11*, 103890–103915. https://doi.org/10.1109/ACCESS.2023.3317371

[15] Sumithra, P., & Thiripurasundari, D. (2017). A review on computational electromagnetics methods. *Advanced Electromagnetics*, *6*(1), 42–55. https://doi.org/10.7716/aem.v6i1.407

[16] Kaur, K., & Sivia, J. S. (2017). A compact hybrid multiband antenna for wireless applications. *Wireless Personal Communications*, *97*(4), 5917–5927. https://doi.org/10.1007/s11277-017-4818-7

[17] Balanis, C. A. (2005). *Antenna Theory: Analysis and Design* (3rd ed.). Wiley-Interscience.

[18] Hasnain, A. A., Nauman, M., Abbas, M., Anwar, M. A., Ahmed, I., & Asghar, M. T. (2020). Simple high gain array antenna for 5G applications. *International Research Journal of Engineering and Technology*, *9*(9), 408–410. https://www.ijert.org/research/simple-high-gain-array-antenna-for-5g-applications-IJERTV9IS090233.pdf

[19] Mahapatra, R. K., Satapathi, G. S., Kumar, P., Shett, A.N., Shettigar, S., & J P, A. (2023). "Design and analysis of microstrip patch antenna. In *Proceedings of the IEEE International Conference on Recent Trends in Electronics and Communication: Upcoming Technologies for Smart Systems (ICRTEC)*, 1–80. https://doi.org/10.1109/ICRTEC56977.2023.10111920

[20] El Issawi, M. L., Konditi, D. B. O., & Usman, A. D. (2024). Design of an enhanced dual-band microstrip patch antenna with defected ground structures for WLAN and WiMax. *Indonesian Journal of Electrical Engineering and Computer Science*, *35*(1), 165–174. https://doi.org/10.11591/ijeecs.v35.i1.pp165-174

[21] Jia, Y., Zhou, S., Wang, Y., Lin, F., & Gao, Z. (2025). A quadratic v-support vector regression approach for load forecasting. *Complex & Intelligent Systems*, *11*(1). https://doi.org/10.1007/s40747-024-01730-7

How to Cite: Hassen, N. A., Tafere, A. A., Hassen, M. R., Mengistu, T. A., Huluka, M. A., & Adgeh, A. T. (2026). Performance Optimization of Multiband Microstrip Antennas Using Support Vector Regression for Wireless Communications. *Archives of Advanced Engineering Science*, *4*(2), 148–159. https://doi.org/10.47852/bonviewAAES52027159